

# SWIPENET: Object detection in noisy underwater images

Long Chen, Feixiang Zhou, Shengke Wang, Junyu Dong, Ning Li, Haiping Ma, Xin Wang and Huiyu Zhou

**Abstract**—In recent years, deep learning based object detection methods have achieved promising performance in controlled environments. However, these methods lack sufficient capabilities to handle underwater object detection due to these challenges: (1) images in the underwater datasets and real applications are blurry whilst accompanying severe noise that confuses the detectors and (2) objects in real applications are usually small. In this paper, we propose a novel Sample-Weighted hyper Network (SWIPENET), and a robust training paradigm named Curriculum Multi-Class Adaboost (CMA), to address these two problems at the same time. Firstly, the backbone of SWIPENET produces multiple high resolution and semantic-rich Hyper Feature Maps, which significantly improve small object detection. Secondly, a novel sample-weighted detection loss function is designed for SWIPENET, which focuses on learning high weight samples and ignore learning low weight samples. Moreover, inspired by the human education process that drives the learning from easy to hard concepts, we here propose the CMA training paradigm that first trains a ‘clean’ detector which is free from the influence of noisy data. Then, based on the ‘clean’ detector, multiple detectors focusing on learning diverse noisy data are trained and incorporated into a unified deep ensemble of strong noise immunity. Experiments on two underwater robot picking contest datasets (URPC2017 and URPC2018) show that the proposed SWIPENET+CMA framework achieves better accuracy in object detection against several state-of-the-art approaches.

**Index Terms**—Underwater object detection, Curriculum Multi-Class Adaboost, sample-weighted detection loss, noisy data.

## I. INTRODUCTION

Autonomous underwater vehicles (AUVs) [1], [2] and remotely operated vehicles (ROVs) [3], [4] equipped with intelligent underwater object detection systems is of great significance for ocean resource exploitation and protection. Unfortunately, complicated underwater environments and lighting conditions introduce considerable noise into the captured images, which has posed massive challenges to intelligent vision-based object detection systems [5], [6], [7]. Therefore, it is crucial to develop novel underwater object detection techniques which effectively handle noise for the AUVs and ROVs applications.

Deep learning based object detection systems have demonstrated promising performance in various applications but still

L. Chen, F. Zhou and H. Zhou are with School of Informatics, University of Leicester, United Kingdom. H. Zhou is the corresponding author (Email: hz143@leicester.ac.uk).

N. Li is with College of Electronic and Information Engineering, Nanjing University of Aeronautics and Astronautics, China.

H. Ma is with Department of Electrical Engineering, Shaoxing University, China.

S. Wang and J. Dong are with Department of information science and engineering, Ocean University of China, China.

X. Wang is with College of Computer and Information, Hohai University, China.

Manuscript received on 1st Oct., 2020; revised xxxxx.

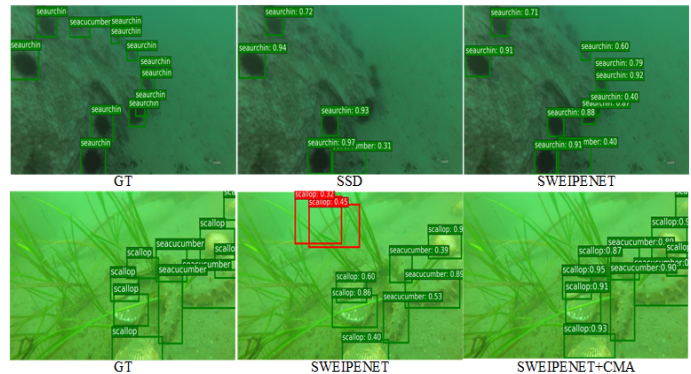


Fig. 1. Exemplar images with ground truth (GT) annotations, results of Single Shot MultiBox Detector (SSD) [8], our proposed SWIPENET and SWIPENET+CMA. The top row shows that SSD cannot detect all the small objects while our proposed SWIPENET outperforms SSD in this case. The bottom row shows our proposed SWIPENET treats the background as objects due to the existence of noisy data while our proposed SWIPENET+CMA performs better than the others.

felt short of dealing with underwater object detection. This is because, firstly, underwater detection datasets are scarce and the objects in the available underwater datasets and real applications are usually small. Current deep learning based detectors cannot effectively detect small objects (see an example shown on top row of Fig. 1). Secondly, the images in the existing underwater datasets and real applications accompany considerable noisy data. It has been known that in the underwater scenes, wavelength-dependent absorption and scattering [9] cause serious visibility loss, contrast decrease and color distortion, resulting in poor imaging of underwater objects and mixture of noisy objects and the background. The noisy data may confuse the deep detector and decrease the generalisation ability of the detector. As shown on the bottom row of Fig. 1, the proposed SWIPENET trained on the noisy data cannot distinguish between the background and the objects.

In this paper, we propose a deep ensemble detector which is effective in dealing with small objects and noisy data in the underwater scenes. To achieve the objectives, we propose a deep backbone network named Sample-Weighted hyper Network (SWIPENET), which fully takes advantage of multiple Hyper Feature Maps. To address the noisy data problem, we propose a novel sample-weighted detection loss function and a novel noise-robust training paradigm named Curriculum Multi-Class Adaboost (CMA), used to train the deep ensemble for underwater object detection. Indeed, the sample-weighted detection loss is used to control the influence of the training samples on SWIPENET. It works with the training paradigm

CMA to train the proposed deep ensemble detector to reduce errors.

The proposed CMA training paradigm is inspired by the idea in the human education system that starts from learning easy tasks, and then gradually increase learning difficulty levels. This learning concept has been utilised to improve the generalisation ability and accelerate convergence in machine learning algorithms [10], [11], [12]. For example, Derenyi et al. [12] reported theoretical analysis where easy examples should be learnt first due to less noise. They treat the samples misclassified by the Bayesian classifier as noisy data and learn the easier samples first, then improve convergence and the generalisation ability. Motivated by these works, our CMA training paradigm consists of two training stages: Noise-eliminating (NECMA) and noise-learning (NLCMA) stages. In the noise-eliminating stage, a 'clean' detector (SWIPENET) of being free from the influence of noisy data is formulated by focusing on learning easy samples whilst ignoring learning hard and noisy data. Then, the previously learnt knowledge by the 'clean' detector is again used to ease the training of the detectors in the noise-learning stage which focuses on learning diverse noisy data. The parameters of the detectors in the noise-learning stage are initialised by those of the 'clean' detector, which help the deep detectors avoiding poor local optimum during training and improving the convergence speed and system generalisation. Finally, to achieve a balance between running time and detection accuracy, we present a selective ensemble algorithm to choose several detectors with a large diversity for the final ensemble. In summary, our contributions can be summarised as follows:

- We propose a novel noise-immune deep detection framework which consists of a backbone network SWIPENET and a powerful training paradigm CMA. The SWIPENET+CMA framework trains a robust deep ensemble detector for the object detection task in the underwater scenes with heterogeneous noisy data and small objects.
- SWIPENET fully takes advantage of both high resolution and semantic-rich Hyper Feature Maps that significantly boost small object detection. Moreover, a novel sample-weighted detection loss is designed for the proposed SWIPENET, which controls the influence of the training samples on SWIPENET according to their weights. We also provide theoretical analysis on the ability of the sample-weighted detection loss in detail.
- To achieve the balance between the detection accuracy and the computational cost, we propose a selective ensemble algorithm to choose the best detector trained with large data diversity.

The rest of the paper is organised as follows. Section II gives a brief introduction about the related work. Section III describes our proposed SWIPENET backbone, CMA training paradigm and selective ensemble algorithm. Section IV describes the experimental set-up and Section V reports the results of the proposed method on two underwater datasets URPC2017 and URPC2018.

## II. RELATED WORK

### A. Underwater object detection

Underwater object detection techniques have been employed in marine ecology studies for many years. Strachan et al. [13] used color and shape descriptors to recognise fish transported on a conveyor belt, monitored by a digital camera. Spampinato et al. [14] presented a vision system for detecting, tracking and counting fish in real-time videos, which consist of video texture analysis, object detection and tracking processes. However, these established methods heavily rely on hand-crafted features, which have a limited representation ability. Choi [15] applied a foreground detection method to extracting candidate fish windows and used Convolution Neural Networks (CNNs) to classify fish species in the field of view. Villon et al. [16] compared a deep learning method against the Histogram of Oriented Gradients (HOG)+Support Vector Machine (SVM) method in detecting coral reef fish, and the experimental results show the superiority of the deep learning methods in underwater object detection. Li et al. [17] exploited Fast RCNN [18] to detect and recognise fish species. Li et al. [19] accelerated fish detection using Faster RCNN [20]. However, the Fast RCNN methods use the features from the last convolution layer of the neural network, which is coarse and cannot effectively detect small objects. In addition, the underwater object detection datasets are extremely scarce that hinders the development of underwater object detection techniques. Recently, Jian et al. [21], [22] proposed the OUC underwater dataset for underwater saliency detection with object-level annotations that can be used to evaluate the exiting systems. Chen et al. [23] further generated high quality reference images for the OUC dataset that provide a fair platform for evaluating different underwater object detection and image enhancement methods.

### B. Sample re-weighting

Sample re-weighting is widely used to address noisy data problems [24] or hard sample mining [25]. It usually assigns a weight to each sample and then optimises the sample-weighted training loss. These can be divided into training loss based and results based methods. For the training loss based sample re-weighting approaches, we may have two research directions. For example, focal loss [26] and hard example mining [25] emphasise on hard samples with high training losses while self-placed learning [27], [28] encourages learning easy samples with low losses. These two possible solutions take different assumptions over the training data. The first solution assumes that hard samples are informative samples and should be learned more, whilst the second one assumes that hard samples are prone to be disturbance or noise. Here, in the underwater object detection tasks, hard samples are probably not useful because they confuse the detector rather than help it. Different from the training loss based sample-reweight methods, Multi-Class Adaboost [29] re-weights the samples according to the classification results. This method focuses on learning misclassified samples by increasing their weights during the iteration. Similarly, we re-weight the samples based on the detection results. This method

seems more intuitive and effective than the training loss based methods.

### C. Curriculum leaning paradigm

In the human education system, it may confuse the learner if s/he directly learns the hard knowledge in the beginning. Instead, the beginner starts from learning easy knowledge while skipping disturbing hard knowledge. In such way, the learning exercise is efficient and effective [30], [31]. This idea is also widely used in many machine leaning algorithms. For example, curriculum learning [32] and self-pace learning [27], [28] are two representatives inspired by the idea of learning easier aspects of the task before moving into a difficult level. Both approaches have been reported to provide better generalisation for the used model. However, Curriculum learning requires the samples in the datasets to be ranked in the order of incremental difficulty levels, but preparing such datasets is not trivial at all in practice. Self-pace learning addresses the sample order issue by training the used model and ranking the samples according to the samples' loss values using the learned model. It assumes the samples with low loss values are easy samples. One major drawback of self-pace learning is that it does not incorporate prior knowledge into the learning and hence loose the generalisation ability. In addition, both methods only train a single model without considering its capacity to learn diverse data. The developed models may be over-fit on some samples and under-fit on other samples.

In this paper, inspired by the human education system, we propose a noise-immune training paradigm CMA that combines the learning tricks from Curriculum Learning and Multi-Class Adaboost. CMA dynamically updates the training samples for the next training iteration based on the previous detection. It first trains a 'clean' detector by gradually reducing the influence of noisy data. Then, it trains multiple detectors by inheriting the knowledge learned by the 'clean' detector. The multiple detectors learning samples with a large diversity are finally selected and combined into a unified noise-immune deep ensemble detector.

## III. PROPOSED METHOD

### A. Sample-Weighted hyPER Network (SWIPENET)

Evidence shows that the down-sampling excises of Convolutional Neural Network result in strong semantics that lead to the success of classification tasks. However, this is not enough for the object detection task which not only needs to recognise the objects but also spatially locates its position. After we have applied several down-sampling operations, the spatial resolutions of the deep layers are too coarse to handle small object detection.

In this paper, we propose the SWIPENET architecture that includes several high resolution and semantic-rich Hyper Feature Maps inspired by Deconvolutional Single Shot Detector (DSSD) [33]. DSSD augments a fast down-sampling detection framework SSD [8] with multiple up-sampling deconvolution layers to increase the resolutions of the feature maps. In the DSSD architecture, firstly, multiple down-sampling

convolution layers are constructed to extract high semantic feature maps that benefit object classification. After several down-sampling operations, the feature maps are too coarse to provide sufficient information for accurate small object localization, therefore, multiple up-sampling deconvolution layers and skip connection are added to recover the high resolutions of the feature maps. However, the detailed information lost in the down-sampling operations cannot be fully recovered even though the resolutions have been recovered. To improve DSSD, we use dilate convolution layers [34], [35] to obtain strong semantics without losing detailed information that support object localization. Fig. 2 illustrates the overview of our proposed SWIPENET, which consists of multiple convolution blocks, dilated convolution blocks, deconvolution blocks and a sample-weighted loss. The front layers of the SWIPENET are based on the architecture of the standard VGG16 model [36] (truncated at the Pool5 layer). Different from DSSD, we add four dilated convolution layers with ReLU activation to the network, which can obtain large receptive fields without sacrificing the resolutions of the feature maps (large receptive fields lead to strong semantics). We further up-sample the feature maps using deconvolution and then add skip connection to pass the fine details of the low layers to the high layers. Finally, we construct multiple Hyper Feature Maps on the deconvolution layers. The prediction of SWIPENET deploys three different deconvolution layers, i.e. Deconv1\_2, Deconv2\_2 and Deconv3\_2 (denoted as Deconvx\_2 in Fig. 2), which increase in size progressively and allow us to predict the objects of multiple scales. At each location of the three deconvolution layers, we define 6 default boxes and use a  $3 \times 3$  convolution kernel to produce  $C + 1$ -D class prediction ( $C$  indicates the number of the object classes and 1 indicates the background class) and 4-D coordinate prediction.

### B. Sample-Weighted detection loss

We propose a novel sample-weighted detection loss function which can model sample weights in SWIPENET. The sample-weighted detection loss enables SWIPENET to focus on learning high weight samples whilst ignoring low weight samples. It cooperates with a novel sample re-weighting algorithm, namely Curriculum Multi-Class Adaboost, to reduce the influence of possible noise on SWIPENET by decreasing their weights.

Following the one-stage deep detector SSD [8], SWIPENET trains an object detector using default boxes on several layers. If the Intersection over Union (IoU) between the default box and its most overlapped object is larger than a pre-defined threshold (0.5 here), then the default box is a match to this object that works as its positive training sample. If a default box does not match any object, it will be regarded as a negative/background training sample. Technically, our sample-weighted detection loss  $L$  consists of a sample-weighted softmax loss  $L_{cls}$  for the bounding box classification and a sample-weighted smooth L1 loss  $L_{reg}$  for the bounding box regression (the derivation of the original softmax loss and

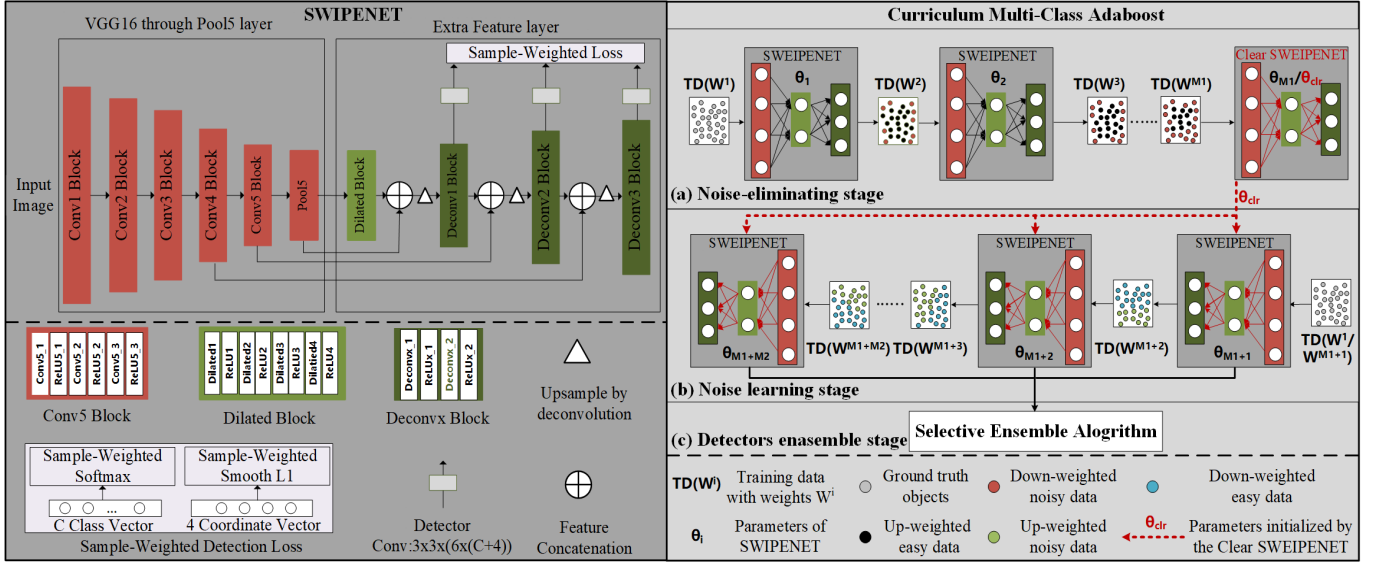


Fig. 2. The overview of our proposed SWIPENET+CMA detection framework. The left shows the structure of our proposed SWIPENET backbone, the right shows the Curriculum Multi-Class Adaboost training paradigm that consist of the (a) Noise-eliminating stage, (b) Noise learning stage, and (c) Detectors ensemble stage.

smooth L1 loss can be found in [8]):

$$L = \frac{\alpha_1}{\bar{N}} L_{cls}(pre\_cls, gt\_cls) + \frac{\alpha_2}{\bar{N}} L_{reg}(pre\_loc, gt\_loc) \quad (1)$$

where  $\bar{N}$  and  $\bar{N}$  are the numbers of all the training samples and positive training samples respectively,  $\alpha_1$  and  $\alpha_2$  denote the weight terms of classification and regression losses respectively.  $L_{cls}$  is the sample-weighted softmax (cross entropy) loss as follows:

$$L_{cls} = - \sum_{i=1}^{\bar{N}} \sum_{c=1}^{C+1} \bar{w}_i^m gt\_cls_i^c \log(pre\_cls_i^c) \quad (2)$$

$$pre\_cls_i^c = \frac{e^{net_i^c}}{\sum_{c=1}^{C+1} e^{net_i^c}} \quad (3)$$

$\bar{w}_i^m$  denotes the sample weight for the  $i$ -th sample computed in the  $m$ -th iteration of CMA in Subsection III-C. CMA adaptively decreases the weights of possible noisy training samples and increases the weights of easy training samples.  $C + 1$  denotes  $C$  object classes plus one background class.  $pre\_cls_i^c$  and  $gt\_cls_i^c$  denote the  $c$ -th element of the predicted outcome and the ground truth class vectors for the  $i$ -th sample.  $gt\_cls_i^c = 1$  if the  $i$ -th sample belongs to the  $c$ -th class,  $gt\_cls_i^c = 0$  otherwise.  $net_i^c$  is the classification prediction from the detection network.

$L_{reg}$  is the sample-weighted smooth L1 loss, formulated as follows:

$$L_{reg} = \sum_{i=1}^{\bar{N}} \sum_{l \in Loc} \bar{w}_i^m Smooth_{L1}(pre\_loc_i^l - gt\_loc_j^l) \quad (4)$$

$$Smooth_{L1}(x) = \begin{cases} 0.5x^2 & \text{if } |x| < 1 \\ |x| - 0.5 & \text{otherwise} \end{cases} \quad (5)$$

$$pre\_loc_i^l = net_i^l, l \in Loc \quad (6)$$

$pre\_loc_i^l$  and  $gt\_loc_i^l$  denote the  $l$ -th element of the predicted and the ground truth coordinate vectors for the  $i$ -th positive training sample respectively.  $Loc = (cx, cy, w, h)$  denotes the relative coordinate information of the object that includes the coordinates of center  $(cx, cy)$  with width  $w$  and height  $h$ .  $net_i^l$  is the coordinate prediction from the detection network.

Here, we investigate how the weight of the sample influences the feature learning of SWIPENET through the sample-weighted detection loss function. Let  $\theta$  be the parameters of SWIPENET, and the gradient of  $L$  with respect to  $\theta$  can be derived as follows:

$$\frac{\partial L}{\partial \theta} = \frac{\alpha_1}{\bar{N}} \frac{\partial L_{cls}}{\partial \theta} + \frac{\alpha_2}{\bar{N}} \frac{\partial L_{reg}}{\partial \theta} \quad (7)$$

To obtain  $\frac{\partial L}{\partial \theta}$ , we first derive  $\frac{\partial L_{cls}}{\partial \theta}$  as

$$\begin{aligned} \frac{\partial L_{cls}}{\partial \theta} &= - \sum_{i=1}^{\bar{N}} \sum_{c=1}^{C+1} \bar{w}_i^m gt\_cls_i^c \frac{\partial \log(pre\_cls_i^c)}{\partial \theta} \\ &= - \sum_{i=1}^{\bar{N}} \sum_{c=1}^{C+1} \bar{w}_i^m gt\_cls_i^c \frac{1}{pre\_cls_i^c} \frac{\partial pre\_cls_i^c}{\partial net_i^c} \frac{\partial net_i^c}{\partial \theta} \end{aligned} \quad (8)$$

where

$$\begin{aligned} \frac{\partial pre\_cls_i^c}{\partial net_i^c} &= \frac{e^{net_i^c} \sum_{c=1}^{C+1} e^{net_i^c} - (e^{net_i^c})^2}{(\sum_{c=1}^{C+1} e^{net_i^c})^2} \\ &= \frac{e^{net_i^c}}{\sum_{c=1}^{C+1} e^{net_i^c}} - \left( \frac{e^{net_i^c}}{\sum_{c=1}^{C+1} e^{net_i^c}} \right)^2 \\ &= pre\_cls_i^c - (pre\_cls_i^c)^2 \end{aligned} \quad (9)$$

Substituting Eq. (9) into Eq. (8), then we have

$$\frac{\partial L_{cls}}{\partial \theta} = \sum_{i=1}^{\bar{N}} \sum_{c=1}^{C+1} \bar{w}_i^m gt\_cls_i^c (pre\_cls_i^c - 1) \frac{\partial net_i^c}{\partial \theta} \quad (10)$$

Secondly, we derive  $\frac{\partial L_{reg}}{\partial \theta}$  as

$$\begin{aligned} \frac{\partial L_{reg}}{\partial \theta} &= \sum_{i=1}^{\tilde{N}} \sum_{l \in Loc} \bar{w}_i^m \frac{\partial Smooth_{L_1}}{\partial pre\_loc_i^l} \frac{\partial pre\_loc_i^l}{\partial net_i^l} \frac{\partial net_i^l}{\partial \theta} \\ &= \begin{cases} \sum_{i=1}^{\tilde{N}} \sum_{l \in Loc} \bar{w}_i^m (pre\_loc_i^l - gt\_loc_j^l) \frac{\partial net_i^l}{\partial \theta} & \text{if } |pre\_loc_i^l - gt\_loc_j^l| < 1 \\ \pm \sum_{i=1}^{\tilde{N}} \sum_{l \in Loc} \bar{w}_i^m \frac{\partial net_i^l}{\partial \theta} & \text{otherwise} \end{cases} \quad (11) \end{aligned}$$

Finally, we have

$$\frac{\partial L}{\partial \theta} = \begin{cases} \frac{\alpha_1}{N} \sum_{i=1}^{\tilde{N}} \sum_{c=1}^{C+1} \bar{w}_i^m gt\_cls_i^c (pre\_cls_i^c - 1) \frac{\partial net_i^c}{\partial \theta} \\ + \frac{\alpha_2}{N} \sum_{i=1}^{\tilde{N}} \sum_{l \in Loc} \bar{w}_i^m (pre\_loc_i^l - gt\_loc_j^l) \frac{\partial net_i^l}{\partial \theta} & \text{if } |pre\_loc_i^l - gt\_loc_j^l| < 1 \\ \frac{\alpha_1}{N} \sum_{i=1}^{\tilde{N}} \sum_{c=1}^{C+1} \bar{w}_i^m gt\_cls_i^c (pre\_cls_i^c - 1) \frac{\partial net_i^c}{\partial \theta} \\ \pm \frac{\alpha_2}{N} \sum_{i=1}^{\tilde{N}} \sum_{l \in Loc} \bar{w}_i^m \frac{\partial net_i^l}{\partial \theta} & \text{otherwise} \end{cases} \quad (12)$$

From Eq. (12), we witness that the gradient of the parameters is influenced by two factors. The first one is the accuracy of the predicted class and coordinates. For the  $i$ -th training sample with ground truth class  $c$  (i.e.,  $gt\_cls_i^c = 1$ ), the closer  $pre\_cls_i^c$  and  $pre\_loc_i^c$  to the ground truth, the smaller the gradients in back-propagation for the  $i$ -th sample. Second, the weights of the samples. Suppose all of the training samples have the same prediction accuracy. The smaller the weight is, the smaller gradient in back-propagation is attached to the  $i$ -th sample. For example, if we assign a weight of 100 and 1 to the same positive sample respectively, then the magnitude of the gradient from the former one may be around 100 times of that of the gradient from the later one. The feature learning of SWIPENET is dominated by high-weight samples while the low-weight samples contribute far less to the update of the CNN features. Hence, the sample-weighted detection loss less counts on the low-weight samples.

### C. Curriculum Multi-class Adaboost (CMA)

Underwater images suffer from the degradation of different levels, e.g. poor lighting, noise and blurs. If we train a detector on the dataset containing severely deteriorated images, the 'noisy data' are easy to confuse the object detector. Such example is illustrated in the bottom of Fig. 1.

Inspired by the human education system that learns from easy to hard samples, we here propose a noise-immune training paradigm, namely Curriculum Multi-class Adaboost (CMA), to train multiple deep detectors and then combine them into a unified ensemble for object detection in the underwater scenes with the data of considerable noise and large diversity. This strategy helps accelerate the convergence and improve the generalisation of the proposed architecture because the detector trained on easy data provides optimum initialisation for the following deep detectors. Good initialisation helps the proposed model to avoid the local optimum problem in training and to improve generalisation, which has been demonstrated in previous work [10], [11], [12].

1) *The overview of the CMA:* CMA is based on Multi-Class Adaboost (MA) [29], which firstly trains multiple base classifiers sequentially and assign a weight value  $\alpha_m$  according to its error rate  $E_m$ . Then, the samples misclassified by the preceding classifier are assigned a higher weight, allowing the

following classifier to focus on learning these samples. Finally, all the weak base classifiers are combined to form an ensemble classifier with corresponding weights.

Different from MA, our proposed CMA algorithm consists of two stages: noise-eliminating (denotes as NECMA) and noise-learning stages (denotes as NLCMA). In each training iteration of NECMA, we reduce the weights of the undetected objects as they are likely to be noisy data [12]. The sample-weighted detection loss enables the next iteration of SWIPENET to focus on learning the high-weight data. By gradually reducing the influence of the noisy data, the generalisation capability of the system is improved and a detector free from the influence of the noisy data is sought. However, after several iterations, the deep detector may over-fit over the easy samples as their weights are too high after several rounds of re-weighting exercises, and the generalisation ability becomes deteriorated. Therefore, we terminate the noise-eliminating stage when the performance does not improve anymore, and the detector/SWIPENET achieving the best detection accuracy is selected as the 'clean' detector that helps the training undertaken in NLCMA. NLCMA focuses on learning diverse noisy samples by increasing their weights. In practice, the parameters of each detector in NLCMA are initialised by those of the 'clean' detector. This strategy effectively alleviates the local optimum problem and significantly accelerate the convergence whilst boosting the generalisation ability.

The proposed CMA training paradigm can be found in Algorithm 1. It iteratively trains  $M$  detectors/SWIPENETs, including  $M_1$  iterations for NECMA and  $M_2$  iterations for NLCMA. We assume the best performing detector (i.e., the 'clean' SWIPENET  $S_{clr}$  parameterised by  $\theta_{clr}$ ) in NECMA is achieved in the  $M_1$ -th iteration,  $M_1$  is experimentally obtained. Denote  $I_{train}$  as the training images with the ground truth objects  $B = \{b_1, b_2, \dots, b_N\}$ ,  $N$  is the number of the objects in the training set,  $b_j = (cls, cx, cy, w, h)$  is the annotation of the  $j$ -th object. We denote  $w_j^m$  as the weight of the  $j$ -th object in the  $m$ -th iteration. Each object's weight is initialised to  $\frac{1}{N}$  in the first iteration, i.e.  $w_j^1 = \frac{1}{N}, j = 1, \dots, N$ .

In the  $m$ -th iteration of CMA, we firstly compute the weights of the positive training samples. If the  $i$ -th positive sample matches the  $j$ -th object during the training, we compute the  $i$ -th positive sample's weight  $\bar{w}_i^m$  using Eq. (13).

$$\bar{w}_i^m = N * w_j^m, 0 < w_j^m < 1 \quad (13)$$

where  $w_j^m$  denotes the weight of the  $j$ -th object in the  $m$ -th iteration. The weight of the positive sample is  $N$  times that of its matched object. This is because the initial weight of each object in CMA is  $\frac{1}{N}$ , and the initial weight of each positive training sample in the sample-weighted detection loss is 1. Secondly, we use the re-weighted samples to train the  $m$ -th detector  $S_m$ . Thirdly, we run the  $m$ -th detector on the training set and receive the detection results  $D_m = \{d_1, d_2, \dots, d_i\}$  while  $d_i = (cls, score, cx, cy, w, h)$  is the  $i$ -th predicted outcome, including the predicted class ( $cls$ ), score ( $score$ ) and coordinates ( $cx, cy, w, h$ ). We compute the  $m$ -th detector's error rate  $E_m$ , based on the percentage of the undetected

---

**Algorithm 1** Noise-immune CMA training paradigm.

**Input:** Training images  $I_{train}$  with ground truth objects  $B = \{b_1, \dots, b_N\}$ , testing images  $I_{test}$ .

**Output:**  $M$  SWIPENETs.

- 1: Initialise the object weights  $w_j^1 = \frac{1}{N}, j = 1, \dots, N$ .
  - 2: **for**  $m = 1$  to  $M_1$  **do**
  - 3:   • Compute the weights of positive samples using Eq. (13).
  - 4:   • Train the  $m$ -th SWIPENET  $G_m$  using Eq. (1).
  - 5:   • Compute the  $m$ -th SWIPENET's error rate  $E_m$  using Eqs. (14)-(15).
  - 6:   • Compute the  $m$ -th SWIPENET's weight  $\alpha_m$  in the ensemble model using Eq. (16).
  - 7:   • Reduce the weights of the undetected objects and increase the weights of the detected objects using Eq. (17).
  - 8: **end for**
  - 9: Obtain the parameter  $\theta_{clr}$  of the  $M_1$ -th SWIPENET.
  - 10: Initialize the object weights  $w_j^{M_1+1} = \frac{1}{N}, j = 1, \dots, N$ .
  - 11: **for**  $m = M_1 + 1$  to  $M_2$  **do**
  - 12:   • Compute the weights of positive samples using Eq. (13).
  - 13:   • Initialize the parameter of the  $m$ -th SWIPENET  $G_m$  using  $\theta_{base}$ .
  - 14:   • Train the  $m$ -th SWIPENET  $G_m$  using Eq. (1).
  - 15:   • Compute the  $m$ -th SWIPENET's error rate  $E_m$  using Eqs. (14)-(15).
  - 16:   • Compute the  $m$ -th SWIPENET's weight  $\alpha_m$  in the ensemble model using Eq. (16).
  - 17:   • Increase the weights of the undetected objects and decrease the weights of the detected objects using Eq. (18).
  - 18: **end for**
  - 19: **return**  $M$  SWIPENETs.
- 

objects.

$$E_m = \sum_{j=1}^N w_j^m I(b_j) / \sum_{j=1}^N w_j^m \quad (14)$$

where

$$I(b_j) = \begin{cases} 0 & \text{if } \exists d \in D_m, \text{ s.t. } b_j.cls == d.cls \wedge IoU(b_j, d) \geq \theta \\ 1 & \text{otherwise} \end{cases} \quad (15)$$

In Eq. (15), if there exists a detection  $d$  which belongs to the same class as the  $j$ -th ground truth object  $b_j$  (i.e.  $b_j.cls == d.cls$ ) and the Intersection over Union (IoU) between the detection and the  $j$ -th object is larger than the threshold  $\theta$  (0.5 here), we set  $I(b_j) = 0$ , indicating the  $j$ -th object has been detected and  $I(b_j) = 1$  is the undetected. Fourthly, we compute the  $m$ -th detector's weight  $\alpha_m$  using Eq. (16), which is used when we ensemble different detectors.

$$\alpha_m = \log \frac{1 - E_m}{E_m} + \log(C - 1) \quad (16)$$

$$w_j^m \leftarrow \frac{w_j^m}{z_m} \exp(\alpha_m (1 - I(b_j))) \quad (17)$$

where  $C$  is the number of the object classes. Finally, we update each object's weight  $w_j^m$  and train the following

detector. In the first  $M_1$  iterations of NECMA, we reduce the weights of the undetected objects by Eq. (17) that enables the next detector to pay less attention to possible noisy data. In the last  $M_2$  iterations of the noise-learning stage, we increase the weights of the undetected objects by Eq. (18), whereas the detector turns to learning the diverse noisy data.  $z_m$  is a normalisation constant. The same iteration repeats again till all  $M$  detectors have been trained.

$$w_j^m \leftarrow \frac{w_j^m}{z_m} \exp(\alpha_m I(b_j)) \quad (18)$$

It is noticed that when CMA changes from NECMA to HLCMA, i.e., in the  $M_1 + 1$ -th iteration, we must re-initialise the weight of each object as  $\frac{1}{N}$ . In each iteration of NLCMA, we initialise the parameter of each detector with the parameter  $\theta_{clr}$  of the 'clean' SWIPENET. These initialisations help the system avoid local maximum (or minimum) problem, whilst efficiently converging to stationary points.

2) *Selective ensemble algorithm:* An ensemble model may be more accurate than a single model, but brings in additional computational overhead. Recent references [37], [38], [39] have pointed out that the ensemble of selective deep models may not only be more compact but also stronger in the generalization ability than that of the overall deep models. To reduce the computational costs, we first select a few detectors trained with large diversity data. If the results of two different detectors look similar, the ensemble model based on the two detectors does not have the complementary ability. We need to determine which detector is used and how many detectors are incorporated in the ensemble model.

We here propose a greedy selection algorithm to select candidate detectors for the final ensemble. Firstly, we construct a candidate ensemble set  $E$  to add up the selected detectors, and initialise it with the detector achieving the highest detection accuracy among all the  $M_2$  detectors as these detectors have not been confused by noisy data. Then, we gradually select a single detector  $D_{m^*}$  having the largest diversity with all the detectors in the ensemble set and add it to the ensemble set, as formulated in Eq. (19).

$$D_{m^*} = \arg \max_{m, D_m \notin E} \sum_{D_n \in E} Q_{mn} \quad (19)$$

Here, we apply the commonly used Q statistic [40] to measuring the diversity of two detectors' performance.

$$Q_{mn} = \frac{N^{11} N^{00} - N^{01} N^{10}}{N^{11} N^{00} + N^{01} N^{10}} \quad (20)$$

$Q_{mn}$  denotes the diversity between the performance of detectors  $D_m$  and  $D_n$ .  $N^{11}$  and  $N^{00}$  are the numbers of the objects detected and missed by the two detectors respectively.  $N^{01}$  is the total number of the objects missed by  $D_m$  and detected by  $D_n$ ,  $N^{10}$  is the total number of the objects detected by  $D_m$  and missed by  $D_n$ . Maximum diversity is achieved at  $Q_{mn} = -1$  when the two detectors make different predictions (i.e.,  $N^{11} = N^{00} = 0$ ), and the minimum diversity is achieved at  $Q_{mn} = 1$  when the two detectors generate identical predictions (i.e.,  $N^{01} = N^{10} = 0$ ).

After all the candidate detectors have been selected, we ensemble them into a unified deep ensemble detector according to their weights computed by Eq. (16) in CMA and their diversity in the ensemble set. We assign a higher weight to the detector with a larger diversity. This enables the ensemble detector to detect diverse objects in the underwater scenes, where a large diversity exists due to the changed illuminations, water depth and object-camera distance. We compute the diversity weight  $div_m$  of detector  $D_m$  as its average diversity with all the detectors in the ensemble set (by Eq. (21)).

$$div_m = \frac{\sum_{D_n \in E, n \neq m} Q_{mn}^*}{(|E| - 1)} \quad (21)$$

The value of  $Q_{mn}$  lies in  $[-1,1]$ . For better representing the weights of the detection model, we normalise  $Q_{mn}$  as  $Q_{mn}^*$  using Eq. (22). The value of  $Q_{mn}^*$  lies in  $[0,1]$ , and the larger diversity the large value of the diversity weight.

$$Q_{mn}^* = 0.5(1 - Q_{mn}) \quad (22)$$

The final weight  $\lambda_i$  of detector  $D_i$  is formulated as

$$\lambda_i = \frac{div_i * \alpha_i}{\sum_{m=1}^{M^*} div_m * \alpha_m} M^*, i = 1, \dots, M^* \quad (23)$$

In the testing stage, we use the weights to re-score the detection boxes.  $M^*$  denotes the number of the selected detectors, and  $M^* / \sum_{m=1}^{M^*} div_m * \alpha_m$  in Eq. (23) is a normalisation term, scaling the score of the box to fall in  $[0,1]$  after re-scoring. In particular, we first run all  $M^*$  selected SWIPENETs on the testing set  $I_{test}$  and produce a  $M^*$  detection set  $Det_m$ .

$$Det_m = D_m(I_{test}), m = 1, 2, \dots, M^* \quad (24)$$

Afterwards, we re-score each detection  $d$  in  $Det_m$  using  $\lambda_m$ .

$$d.score = \lambda_m d.score, d \in Det_m \quad (25)$$

Finally, we combine all the detections and utilise Non-Maximum Suppression [41] to remove the overlapped detections by Eq. (26), resulting in the final detection results  $Det$ .

$$Det = NonMaximumSuppression(\bigcup_{m=1}^{M^*} Det_m) \quad (26)$$

## IV. EXPERIMENTS SETUP

To demonstrate the effectiveness of the proposed method, we conduct comprehensive evaluations on two underwater datasets URPC2017 and URPC2018 from the Underwater Robot Picking Contest (detailed descriptions of the contest are provided in the Supplementary). In this section, we first introduce the experimental datasets and evaluation metrics. Then, we describe the implementation details.

### A. Datasets

We evaluate our approach against two underwater datasets URPC2017 and URPC2018 from the Underwater Robot Picking Contest. The URPC2017 dataset has 3 object categories, including seacucumber, seaurchin and scallop. There are 18,982 training images and 983 testing images. The

URPC2018 dataset has 4 object categories, including seacucumber, seaurchin, scallop and starfish. There are 2,897 images in the training set, but the testing set is not publicly available. We randomly split the training set of URPC2018 into a training set of 1,999 images and a testing set of 898 images. Both two datasets provide underwater images and box level annotations.

### B. Implementation details

All the experiments are conducted on a server with an Intel Xeon CPU @ 2.40GHz and a single Nvidia Tesla P100 GPUs with a 16 GB memory. For our proposed detection framework, we implement it using the Keras framework, and train it with the Adam optimisation algorithm. We use an image scale of 512x512 as the input for both training and testing. On URPC2017, the batch-size is 16, and the learning rate is 0.0001. Our models often diverge when we use a high learning rate due to unstable gradients, and all the detectors in the ensemble achieve the best performance after running 120 epochs. On URPC2018, the batch-size is 16. We first train each detector in the ensemble with a learning rate 0.001 for 80 epochs, and then train them with a learning rate 0.0001 for another 40 epochs. The source code will be made available at: <https://github.com/LongChenCV/SWIPENET+CMA>.

## V. RESULTS AND DISCUSSION

In this section, we present and discuss the experimental results and findings. We first conduct the ablation experiments to investigate the influence of different components on our SWIPENET+CMA framework, including the skip connection, the dilated convolution layers and the CMA training paradigm (consisting of NECMA and NLCMA). Then, we compare our method against several state-of-the-art detection frameworks on URPC2017 and URPC2018, including IMA [42], SSD [8], YOLOv3 [43] and Faster RCNN [20]. Finally, we compare our proposed CMA with several representative training paradigms to demonstrate its effectiveness on dealing with noisy data.

### A. Ablation studies on the skip connection and dilated convolution layer.

TABLE I  
ABLATION STUDIES ON URPC2017 AND URPC2018. SKIP INDICATES SKIP CONNECTION, AND DILATION INDICATES DILATED CONVOLUTION LAYER. MAP INDICATES MEAN AVERAGE PRECISION(%).

Dataset	Network	Skip	Dilation	mAP
URPC2017	UWNET1		✓	40.4
	UWNET2			38.3
	SWIPENET	✓	✓	42.1
URPC2018	UWNET1		✓	61.2
	UWNET2			58.1
	SWIPENET	✓	✓	62.2

To investigate the influence of skip connection, we design the first baseline network UWNET1 which has the same structure as SWIPENET except that it does not contain skip connection between the low and high layers. The second network UWNET2 replaces the four dilated convolution layers in UWNET1 with standard convolution layers to learn

TABLE II  
THE PERFORMANCE (MAP(%)) OF SWIPENET IN EACH ITERATION OF CMA ON TEST SET OF URPC2017 AND URPC2018.

Dataset	Stage	NECMA					NLCMA						
		Iteration	1	2	3	4	5	1	2	3	4	5	6
URPC2017	Single	42.1	44.2	45.3	40.5	37.2	47.5	47.2	46.2	47.9	<b>48.0</b>	47.0	47.6
	Ensemble	42.1	45.0	46.3	45.3	44.2	47.5	48.6	49.8	52.3	<b>52.5</b>	52.5	52.5
URPC2018	Single	62.2	63.3	62.4	61.2	59.3	65.0	64.8	<b>65.3</b>	64.5	64.5	63.9	64.3
	Ensemble	62.2	64.5	64.0	62.8	62.1	65.0	65.4	66.9	67.5	<b>68.0</b>	68.0	68.0

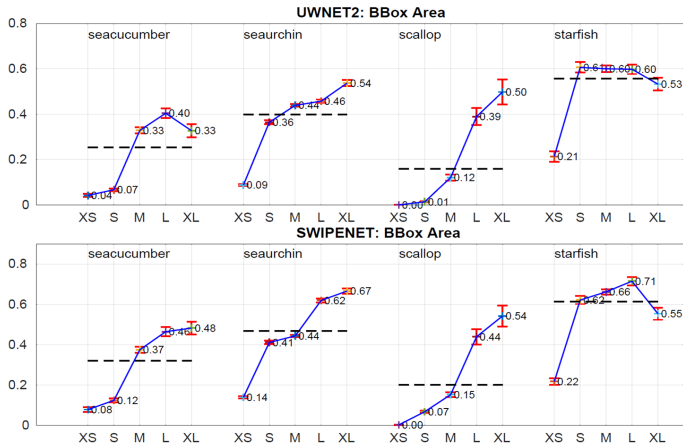


Fig. 3. The mean Average Precision of UWNET2 and SWIPENET for objects with different object sizes. The object size is measured as the pixel area of the bounding box. XS (bottom 10%)=extra-small; S (next 20%)=small; M (next 40%)=medium; L (next 20%)=large; XL (next 10%)=extra-large.

the influence of the dilated convolution. Table I shows the performance comparison of different networks on URPC2017 and URPC2018. SWIPENET holds 1.7% and 1.0% better than UWNET1 on the two datasets respectively. The gains come from the skip connection which passes fine detailed information of the lower layers such as object boundary to the high layers that are important for object localisation. Compared to UWNET2, UWNET1 performs 2.1% and 3.1% improvement because the dilated convolution in UWNET1 brings much semantic information to the high layers which enhances the classification ability. We also present the mean Average Precision of UWNET2 and SWIPENET for the objects with different sizes on URPC2018, shown in Fig. 3, from which we can see the skip connection and dilated convolution layer largely improves the small object detection accuracy. For example, for small objects (S) of seacucumber, seaurchin and scallop categories, SWIPENET improves 5%~6% mAP over UWNET2.

### B. Ablation studies on CMA

In this subsection, we investigate the influence of CMA (including NECMA and NLCMA) on the final detection results. In our experiments, the number of the iterations of NECMA is set to 5 and the number of the iterations of NLCMA is set to 7. Table II shows the performance of the single model and the ensemble model after each iteration on the testing set of URPC2017 and URPC2018.

**The role of NECMA.** From Tables II, in the noise-eliminating stage (NECMA), we can see that the 'clean' SWIPENET (also the best performing single detector) is achieved in the 3rd iteration on URPC2017 and in the 2nd iteration on URPC2018. So we set  $M_1 = 3$  on URPC2017 and  $M_1 = 2$  on URPC2018. Both 'clean' SWIPENETs perform much better than the detectors in the 1st iteration. We assume this is because the noisy data which are extremely similar to the backgrounds confuse the detectors in the 1st iteration. Fig. 5 shows the top three false positives for the 1st detector on URPC2017 and URPC2018, we can see that the background error (detecting the backgrounds as the objects) has much influenced on the false positives than the localisation error. To further verify this assumption, we use the detection analysis tool of [44] to analyse the false positives of the 1st detector and the 'clean' detector in NECMA. Fig. 4 shows the distribution of the top-ranked false positives for each category of URPC2017 and URPC2018. We can see that the 1st detector cannot well distinguish the objects with complex background and generate much more background errors than the 'clean' detector. NECMA gradually reduces the influence of the noisy data on the single detector by decreasing their weights, and the background error clearly decreases in the detection results of the 'clean' SWIPENET.

However, the performance of the single detector is less satisfactory. This is because most of the detected objects are continuously up-weighted and the object detectors over-fit over these high-weight objects. Regarding the ensemble detector, we observe that it has better performance than the single detector on the two datasets. The NECMA algorithm gives the best deep ensemble detector 4.2% and 2.3% improvement on the two datasets, respectively.

**The role of NLCMA.** In the noise-learning stage (NLCMA), we initialise each detector using the parameter learned in the 'clean' detector. This strategy provides a good initialisation for the following detectors which avoid getting stuck in poor local minima during the training. With this initialisation strategy, the detectors converge much faster during the training on URPC2018, shown in Fig. 6 (we also take the testing set as the validation set and investigate the influence of this initialisation strategy on the validation loss). From Table II, we can see all the detectors in the NLCMA stage perform better than the 'clean' detectors on the two datasets. This is because the detectors in NLCMA are able to well detect the noisy target with the help of the 'clean' detector. The fundamental knowledge learnt by the 'clean' detector helps the following detectors identify the minor discrepancies between the noisy targets and the backgrounds. The best single detector



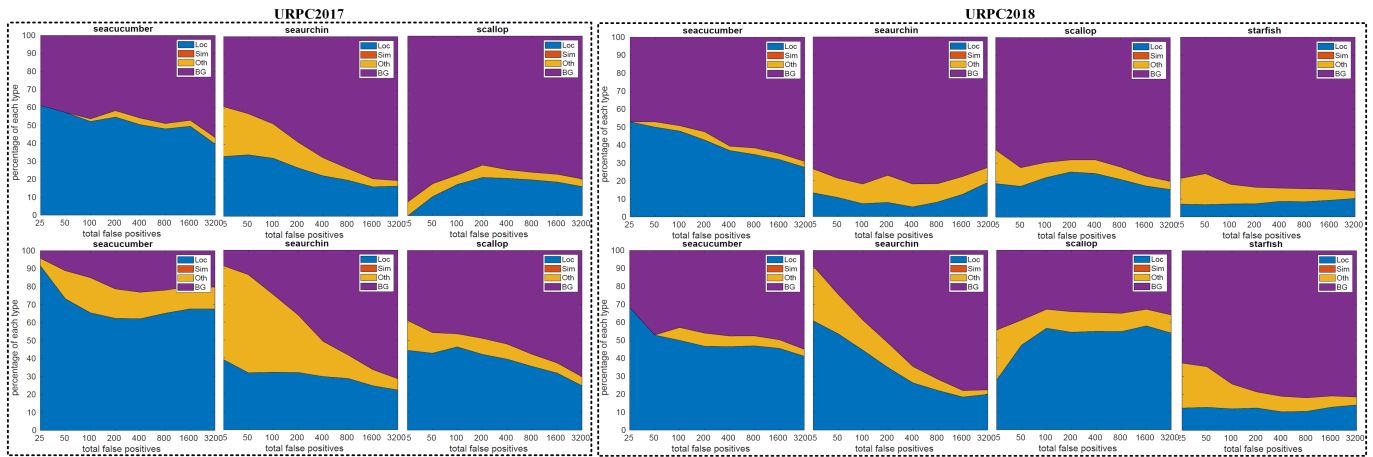


Fig. 4. The distribution of top-ranked false positive types of the 1st detector in NECMA for each category on URPC2018. The false positive types include localisation error (Loc), confusion with similar categories (Sim), with or with background (BG). The top row shows the results of the 1st SWIPENET and the bottom row shows the results of ‘clean’ SWIPENET.

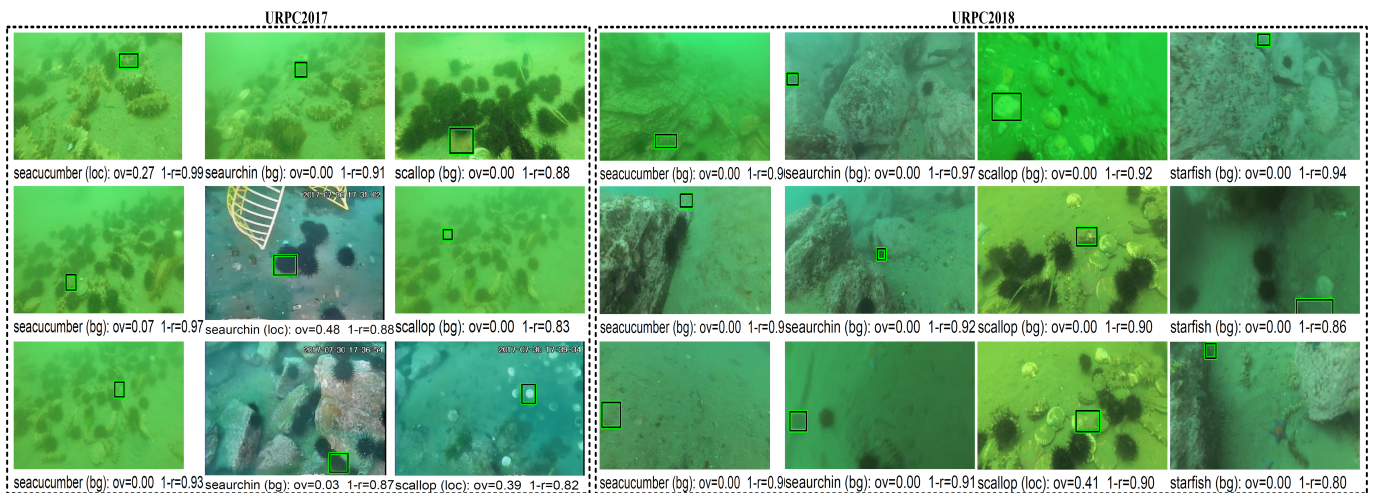


Fig. 5. Examples of top false positives: We show the top three false positives (FPs) for all categories on URPC2017 and URPC2018. The text indicates the type of error (“loc”=localization; “bg”=confusion with backgrounds), the amount of overlap (“ov”) with a true object, and the fraction of correct examples that are ranked lower than the given false positive (“1-r”, for 1-recall). Localization errors are due to insufficient overlaps (less than 0.5).

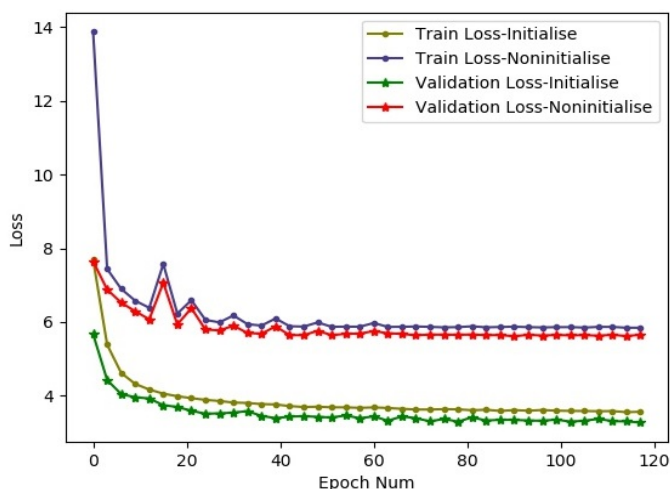


Fig. 6. The learning curve of SWIPENETs with and without initialisation by the ‘clean’ SWIPENET.

is achieved in the 5th iteration of NLCMA on URPC2017 and in the 3rd iteration of NLCMA on URPC2018. The best ensemble detector is achieved in the 5th iteration of NLCMA on the two datasets. After the 5th iteration, the performance of the ensemble detector keep stable because the following single detectors are overlapped with previous single detectors in terms of detection results. Hence, we set  $M_2 = 5$  for the two datasets.

### C. Ablation studies on the selective ensemble algorithm.

We investigate the selective ensemble algorithm for its detection performance. Fig. 7 shows the performance of the ensemble detector with different numbers of the selected detectors. The ensemble detector without the selective ensemble algorithm achieves the best detection accuracy when we ensemble five detectors. The ensemble detector with the selective ensemble algorithm achieves the same detection accuracy by integrating only three selected detectors on URPC2017 and two selected detectors on URPC2018. This demonstrates some

TABLE III  
COMPARISON WITH THE STATE-OF-ARTS ON URPC2017.

Dataset		URPC2017				URPC2018				
Methods	Backbone	seacucumber	seaurchin	scallop	mAP	seacucumber	seaurchin	scallop	starfish	mAP
SSD300	VGG16	28.1	51.3	21.2	33.5	38.5	83.0	30.8	75.1	56.9
SSD512	VGG16	38.4	52.9	15.7	35.7	44.2	84.4	35.8	78.1	60.6
YOLOv3	DarkNet53	28.4	50.3	22.4	33.7	35.7	83.0	34.0	77.9	57.7
Faster RCNN	VGG16	27.2	45.0	31.9	34.7	43.3	83.0	32.0	74.5	58.2
Faster RCNN	ResNet50	31.0	41.4	33.5	35.3	41.1	83.2	34.5	77.2	59.0
Faster RCNN	ResNet101	26.2	47.7	32.5	35.5	44.3	82.5	34.7	77.5	59.8
IMA [42]	SWIPENET	44.4	52.4	42.1	46.3	52.8	84.1	42.9	78.0	64.5
OurFirstSingle	SWIPENET	43.6	51.3	31.2	42.1	46.4	84.0	40.2	78.2	62.2
OurClearSingle	SWIPENET	45.0	49.7	41.3	45.3	50.3	83.7	39.8	79.4	63.3
OurBestSingle	SWIPENET	46.6	55.8	41.6	48.0	54.8	81.5	46.6	78.4	65.3
OurCMA	SWIPENET	<b>49.1</b>	<b>62.3</b>	<b>46.1</b>	<b>52.5</b>	<b>56.4</b>	<b>84.6</b>	<b>50.9</b>	<b>79.9</b>	<b>68.0</b>

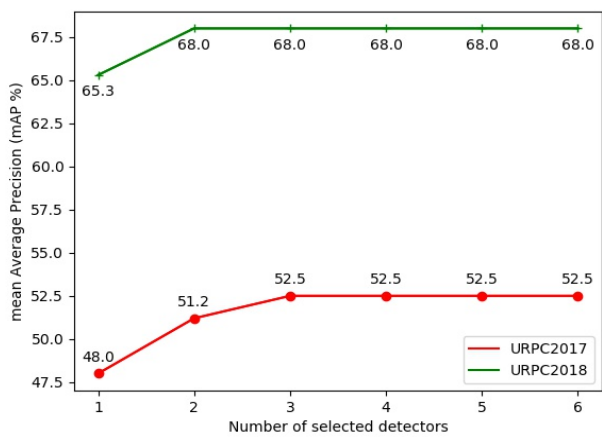


Fig. 7. The performance of the ensemble with different numbers of detectors.

of the detectors do not help boosting the final performance in the ensemble. Few detectors with large diverse data are sufficient to achieve the best performance. The selective ensemble algorithm surely helps reduce the computational overhead during testing due to the reduced number of the detectors.

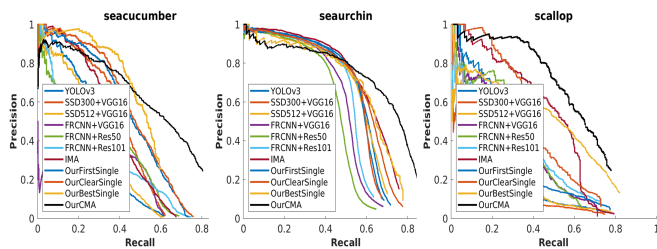


Fig. 8. Precision/Recall curves of different detection methods on URPC2017.

#### D. Comparison with state-of-the-art detection frameworks

In this section, we compare our proposed deep detector with other state-of-the-art detection frameworks, including IMA [42], SSD [8], YOLOv3 [43] and Faster RCNN [20].

**Implementation details.** For SSD, we use VGG16 [36] as the backbone network and conduct experiments on two SSD with different input sizes, i.e. SSD300 and SSD512. For Faster

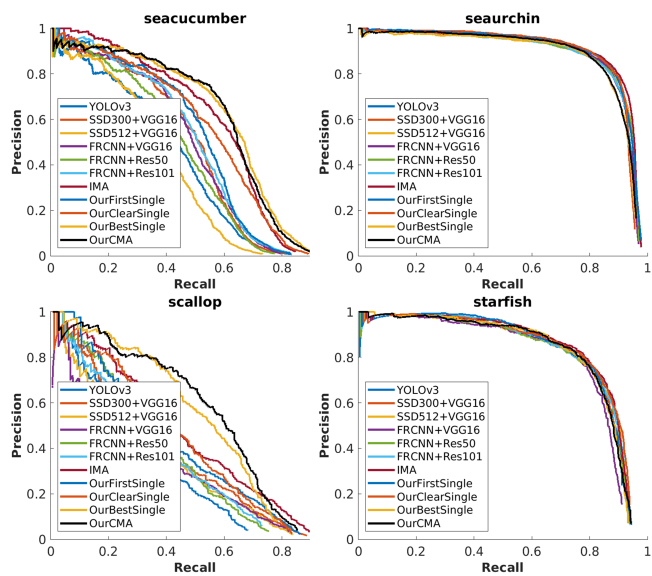


Fig. 9. Precision/Recall curves of different detection methods on URPC2018.

RCNN, we use three backbone networks including VGG16, ResNet50 [45] and ResNet101 [45]. For YOLOv3, we use its original DarkNet53 network. The comparison methods are tuned to have the best performance.

Tables III shows the experimental results on URPC2017 and URPC2018. On URPC2017, SSD512 achieves 35.7% mAP, which improves 2.2% over SSD300. The gain comes from the increase of the input size. In SSD512, more default object scales and higher resolution feature maps are used for detection due to the large input size. On the high resolution feature maps, more features can be extracted for small objects that benefit the detection of small objects. Faster RCNN with ResNet101 performs better than Faster RCNN with ResNet50 and VGG16, where the deeper backbone ResNet101 plays a critical role. In addition, SSD512 achieves better performance than Faster RCNN, even though Faster RCNN uses ResNet101 as the backbone network which has better performance than VGG16. It is because SSD512 detects multi-scale objects on different layers, and performs better than Faster RCNN on small object detection. OurFirstSingle, the SWIPENET, trained in the 1st iteration of CMA, outperforms the other backbones based frameworks by a large margin

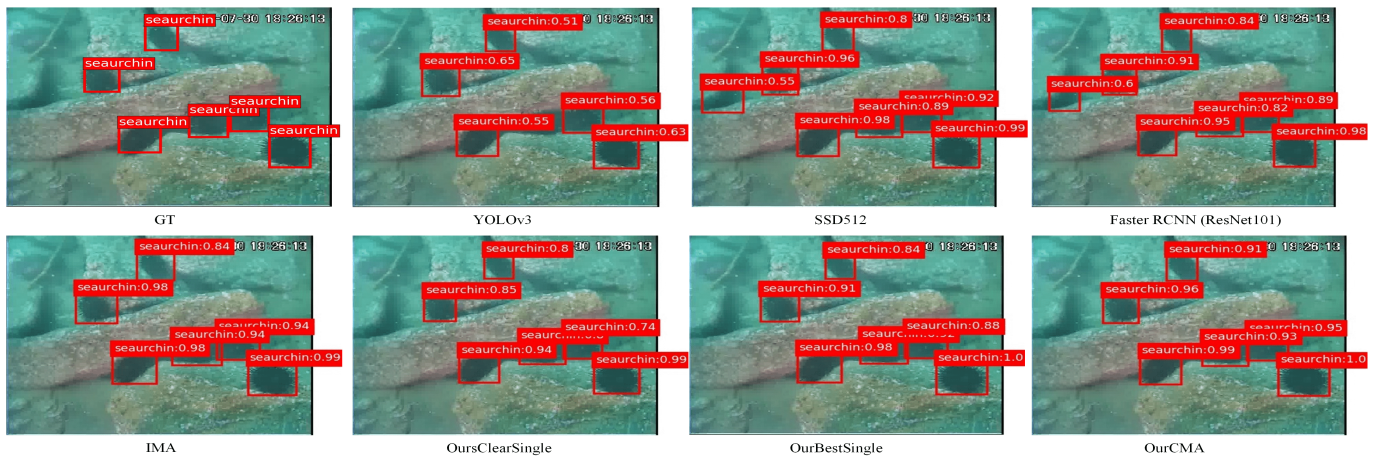


Fig. 10. Visualization of object detection results of different detection frameworks on URPC2017.

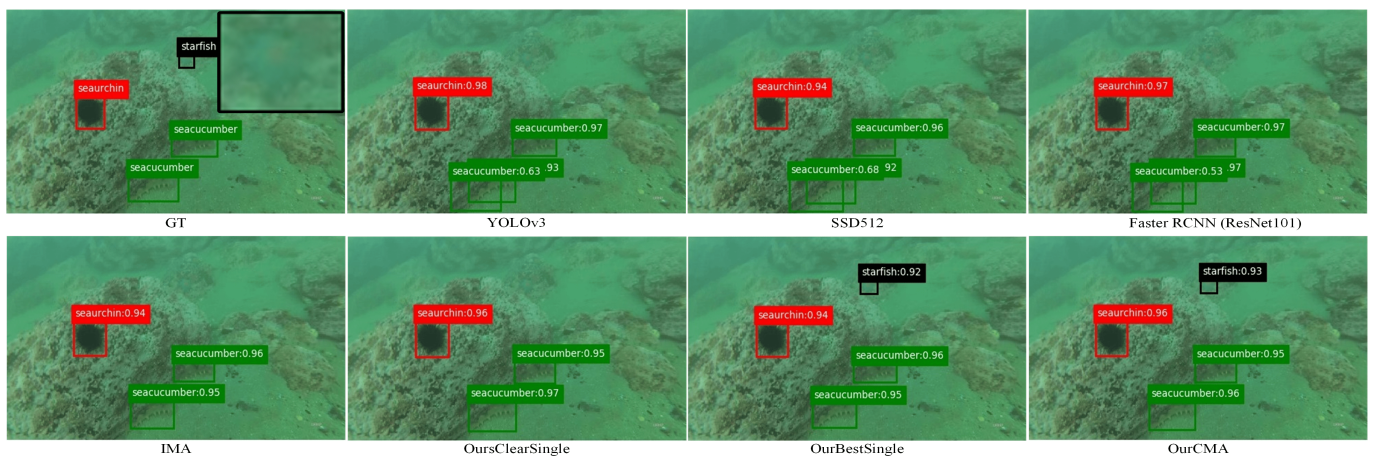


Fig. 11. Visualization of object detection results of different detection frameworks. GT denotes the image with ground truth annotations, and the top left black box shows a starfish that looks extremely similar to the background.

(above 6.4%) on URPC2017, demonstrating the superiority of our proposed SWIPENET backbone in detecting small objects. By reducing the influence of the noisy data, OurClearSingle, the 'clean' single SWIPENET, improves 3.2% over OurFirstSingle. OurBestSingle, the best performing single SWIPENET, achieves 48.0% mAP, and performs even better than the deep ensemble SWIPENET trained with the IMA algorithm. This is because SWIPENET+IMA ignores learning the noisy data and hence it cannot detect most of the noisy data during testing. Benefiting from the CMA training paradigm, OurCMA further improves the results to 52.5% mAP. The gain comes from its capacity to detect the diverse noisy data. Fig. 8 shows the Precision/Recall curves of different detection methods on URPC2017. OurCMA (black curve) has the best performance on the overall object categories of URPC2017.

On URPC2018, OurFirstSingle with SWIPENET backbone achieves 62.2% mAP and outperforms the detection frameworks with other backbones. OurClearSingle improves 1.1% over OurFirstSingle, and OurBestSingle achieves the best single detector's performance, 65.3% mAP. OurCMA outperforms all the other state-of-the-art methods by a large margin, demonstrating its superiority in detecting small objects

and handling noisy data. Fig. 9 shows the Precision/Recall curves of different detection methods on URPC2018. OurCMA performs the best on the overall object categories of URPC2018. It is also worth noting that, all the methods achieves higher detection accuracy on URPC2018 than that on URPC2017, because the images of URPC2017 are far more noisy than those of URPC2018. In addition, many objects in the images of URPC2017 are mislabelled or incorrectly labelled due to the extremely low visibility. Figs. 10 and 11 shows the detection results of an exemplar underwater image on URPC2017 and URPC2018. YOLOv3, SSD512 and Faster RCNN (ResNet101) usually mis-detected the background as the object, because the noisy data, for example the starfish in GT of Fig 11, are extremely similar to the background and confuses the detector. By reducing the influence of the noise during training, IMA and OurClearSingle can effectively distinguish the background from the noisy data. However, both of them are unable to handle severe noisy data. OurCMA and OurBestSingle focus on learning the noisy data in the NLMA stage, and hence are able to detect targets from the severe noisy data.

TABLE IV  
THE PERFORMANCE (MAP(%)) OF SWIPENET IN EACH ITERATION OF DIFFERENT TRAINING PARADIGM ON THE TEST SET OF URPC2017 AND URPC2018.

Dataset	Iteration	1	2	3	4	5	6	7
URPC2017	SWIPENET+CMA	47.5	48.6	49.8	52.3	<b>52.5</b>	52.5	52.5
	SWIPENET+MA	<b>42.1</b>	41.0	40.5	39.2	39.5	38.8	40.2
	SWIPENET+Curriculum	42.1	41.0	<b>43.9</b>	-	-	-	-
	SWIPENET+Anti-Curriculum	<b>42.1</b>	40.8	41.4	-	-	-	-
URPC2018	SWIPENET+CMA	65.0	65.4	66.9	67.5	<b>68.0</b>	68.0	68.0
	SWIPENET+MA	<b>62.2</b>	62.0	61.0	61.2	60.1	58.8	60.2
	SWIPENET+Curriculum	62.2	62.1	<b>63.8</b>	-	-	-	-
	SWIPENET+Anti-Curriculum	<b>62.2</b>	56.9	58.2	-	-	-	-

### E. Comparison with representative learning paradigms

We conduct additional experiments to further compare our CMA learning paradigm with several representative learning paradigms, including Multi-Class Adaboost (MA) [42], Curriculum [32], and Anti-Curriculum.

**Implementation details.** Different from CMA, MA ensembles multiple detectors focusing on learning undetected hard samples by up-weighting their weights. We design the comparison experiments for MA and Anti-Curriculum which focus on leaning hard samples. In the underwater object detection task, we find these hard samples may be noisy and confuse the detectors instead of helping. The Curriculum paradigm needs to define the easy and hard training samples: Similar to [12] that takes misclassified samples as the hard samples, we take the undetected objects as hard samples and the detected objects as easy samples. We first use the detector, trained on all the training data, to split the training data into easy and hard samples, i.e., the detected objects as easy and undetected objects as hard samples. Then, we train a single detector on the easy samples and fine-tune the detector on the hard samples. Inversely, for the Anti-Curriculum paradigm, we train a single detector on the hard samples and fine-tune the detector on the easy samples. Technically, we set the weights of the non-training samples as '0' and the weights of the training samples as '1', where our sample-weighted detection loss links to the samples with weight '1' with no connection with the samples of weight '0'.

Table IV shows the performance comparison of different training paradigms. Our CMA performs much better than the other training paradigms, achieving the best 52.5% mAP and 68.0% mAP on the two datasets. After the 1st iteration, MA and Anti-Curriculum enable the detectors to focus on learning the noisy data that degrade the system performance. This is because the noisy data confuse the detectors which are unable to distinguish the minor differences existing between the noisy data and the backgrounds. On the two datasets, Curriculum decays the performance in the 2nd iteration but boosts the performance in the 3rd iteration. This is because Curriculum trains the detectors using insufficient easy samples in the 2nd iteration. After having fine-tuned over the remaining hard samples, the performance improves and achieves better than that in the 1st iteration. The gains come from the easy-to-hard training strategy and sufficient training data. However, we find CMA still performs much better than Curriculum (8.6% and 4.2% better on URPC2017 and URPC2018 respectively).

This is because the underwater datasets contain considerable diverse data resources due to frequently changing illuminations and environments, the ensemble model is able to learn diverse data and performs much better than the single model trained using the Curriculum paradigm whose generalisation ability is limited.

## VI. CONCLUSION

This paper offers a compelling insight on the training strategy of deep detectors in underwater scenes where noisy data exist. We have presented a new neural network architecture, called Sample-Weighted hyper Network (SWIPENET), for small underwater object detection. Moreover, a sample re-weighting algorithm named Curriculum Multi-Class Adaboost (IMA) had been presented to deal with the noise issue. Our proposed method achieved the state-of-the-art performance on the challenging datasets, with time complexity of  $M$  times higher than a single model (since it is an ensemble of  $M$  deep neural networks). Hence, in our future work, reducing the computational complexity of our proposed method is of vital importance. In addition, current deep models introduce attention mechanisms and novel loss functions to handle the issues of noise and small objects detection.

## ACKNOWLEDGMENT

Thanks for National Natural Science Foundation of China and Dalian Municipal People's Government providing the underwater object detection datasets for research purposes. This project of underwater object detection is supported by China Scholarship Council and Zhejiang Provincial Natural Science Foundation of China under Grant No. LY19F030011.

## REFERENCES

- [1] Sahoo, A., Dwivedy, S. K., and Robi, P. S. (2019). Advancements in the field of autonomous underwater vehicle. *Ocean Engineering*, 181, 145-160.
- [2] Carlucho, I., De Paula, M., Wang, S., Petillot, Y., and Acosta, G. G. (2018). Adaptive low-level control of autonomous underwater vehicles using deep reinforcement learning. *Robotics and Autonomous Systems*, 107, 71-86.
- [3] Muzert, E., Welker, K., Cooper, I., Bittleston, S., Combee, L., Ross, R., and Kotochigov, E. (2015). U.S. Patent No. 9,013,952. Washington, DC: U.S. Patent and Trademark Office.
- [4] Macreadie, P. I., McLean, D. L., Thomson, P. G., Partridge, J. C., Jones, D. O., Gates, A. R., ... and Techera, E. (2018). Eyes in the sea: unlocking the mysteries of the ocean using industrial, remotely operated vehicles (ROVs). *Science of the Total Environment*, 634, 1077-1091.

- [5] Liu, R., Fan, X., Zhu, M., Hou, M., and Luo, Z. (2020). Real-world underwater enhancement: Challenges, benchmarks, and solutions under natural light. *IEEE Transactions on Circuits and Systems for Video Technology*.
- [6] Zhou, Y., Wu, Q., Yan, K., Feng, L., and Xiang, W. (2018). Underwater image restoration using color-line model. *IEEE Transactions on Circuits and Systems for Video Technology*, 29(3), 907-911.
- [7] Ye, X., Li, Z., Sun, B., Wang, Z., Xu, R., Li, H., and Fan, X. (2019). Deep Joint Depth Estimation and Color Correction from Monocular Underwater Images based on Unsupervised Adaptation Networks. *IEEE Transactions on Circuits and Systems for Video Technology*.
- [8] Liu, W., Anguelov, D., Erhan, D., Szegedy, C., Reed, S., Fu, C. Y., and Berg, A. C. (2016, October). Ssd: Single shot multibox detector. In *European Conference on Computer Vision* (pp. 21-37). Springer, Cham.
- [9] Akkaynak, D., and Treibitz, T. (2018). A revised underwater image formation model. In *Proceedings of the IEEE Conference on Computer Vision and Pattern Recognition* (pp. 6723-6732).
- [10] Hanin, B., and Rolnick, D. (2018). How to start training: The effect of initialization and architecture. In *Advances in Neural Information Processing Systems* (pp. 571-581).
- [11] Mishkin, D., and Matas, J. (2015). All you need is a good init. *arXiv preprint arXiv:1511.06422*.
- [12] Derényi, I., Geszti, T., and Györgyi, G. (1994). Generalization in the programmed teaching of a perceptron. *Physical Review E*, 50(4), 3192.
- [13] Strachan, N. J. C. (1993). Recognition of fish species by colour and shape. *Image and Vision Computing*, 11(1), 2-10.
- [14] Spampinato, C., Chen-Burger, Y. H., Nadarajan, G., and Fisher, R. B. (2008). Detecting, Tracking and Counting Fish in Low Quality Unconstrained Underwater Videos. *VISAPP* (2), 2008(514-519), 1.
- [15] Choi, S. (2015). Fish Identification in Underwater Video with Deep Convolutional Neural Network: SNUMedinfo at LifeCLEF Fish task 2015. In *CLEF (Working Notes)*.
- [16] Villon, S., Chaumont, M., Subsol, G., Villéger, S., Claverie, T., and Mouillot, D. (2016, October). Coral reef fish detection and recognition in underwater videos by supervised machine learning: Comparison between Deep Learning and HOG+SVM methods. In *International Conference on Advanced Concepts for Intelligent Vision Systems* (pp. 160-171). Springer, Cham.
- [17] Li, X., Shang, M., Qin, H., and Chen, L. (2015, October). Fast accurate fish detection and recognition of underwater images with fast r-cnn. In *OCEANS 2015-MTS/IEEE Washington* (pp. 1-5). IEEE.
- [18] Girshick, R. (2015). Fast r-cnn. In *Proceedings of the IEEE International Conference on Computer Vision* (pp. 1440-1448).
- [19] Li, X., Shang, M., Hao, J., and Yang, Z. (2016, April). Accelerating fish detection and recognition by sharing CNNs with objectness learning. In *OCEANS 2016-Shanghai* (pp. 1-5). IEEE.
- [20] Ren, S., He, K., Girshick, R., and Sun, J. (2015). Faster r-cnn: Towards real-time object detection with region proposal networks. In *Advances in Neural Information Processing Systems* (pp. 91-99).
- [21] Jian, M., Qi, Q., Dong, J., Yin, Y., Zhang, W., and Lam, K. M. (2017, July). The OUC-vision large-scale underwater image database. In *2017 IEEE International Conference on Multimedia and Expo (ICME)* (pp. 1297-1302). IEEE.
- [22] Jian, M., Qi, Q., Dong, J., Yin, Y., and Lam, K. M. (2018). Integrating QDWD with pattern distinctness and local contrast for underwater saliency detection. *Journal of Visual Communication and Image Representation*, 53, 31-41.
- [23] Chen, L., Tong, L., Zhou, F., Jiang, Z., Li, Z., Lv, J., ... and Zhou, H. (2020). A Benchmark dataset for both underwater image enhancement and underwater object detection. *arXiv preprint arXiv:2006.15789*.
- [24] Ren, M., Zeng, W., Yang, B., and Urtasun, R. (2018). Learning to reweight examples for robust deep learning. *arXiv preprint arXiv:1803.09050*.
- [25] Shrivastava, A., Gupta, A., and Girshick, R. (2016). Training region-based object detectors with online hard example mining. In *Proceedings of the IEEE Conference on Computer Vision and Pattern Recognition* (pp. 761-769).
- [26] Lin, T. Y., Goyal, P., Girshick, R., He, K., and Dollár, P. (2017). Focal loss for dense object detection. In *Proceedings of the IEEE International Conference on Computer Vision* (pp. 2980-2988).
- [27] Kumar, M. P., Packer, B., and Koller, D. (2010). Self-paced learning for latent variable models. In *Advances in Neural Information Processing Systems* (pp. 1189-1197).
- [28] Ghasedi, K., Wang, X., Deng, C., and Huang, H. (2019). Balanced self-paced learning for generative adversarial clustering network. In *Proceedings of the IEEE Conference on Computer Vision and Pattern Recognition* (pp. 4391-4400).
- [29] Hastie, T., Rosset, S., Zhu, J., and Zou, H. (2009). Multi-class adaboost. *Statistics and its Interface*, 2(3), 349-360.
- [30] Altmann, G. T. (2002). Learning and development in neural networks—the importance of prior experience. *Cognition*, 85(2), B43-B50.
- [31] Rohde, D. L., and Plaut, D. C. (1999). Language acquisition in the absence of explicit negative evidence: How important is starting small?. *Cognition*, 72(1), 67-109.
- [32] Bengio, Y., Louradour, J., Collobert, R., and Weston, J. (2009, June). Curriculum learning. In *Proceedings of the 26th Annual International Conference on Machine Learning* (pp. 41-48).
- [33] Fu, C. Y., Liu, W., Ranga, A., Tyagi, A., and Berg, A. C. (2017). Dssd: Deconvolutional single shot detector. *arXiv preprint arXiv:1701.06659*.
- [34] Chen, L. C., Papandreou, G., Kokkinos, I., Murphy, K., and Yuille, A. L. (2014). Semantic image segmentation with deep convolutional nets and fully connected crfs. *arXiv preprint arXiv:1412.7062*.
- [35] Yu, F., Koltun, V., and Funkhouser, T. (2017). Dilated residual networks. In *Proceedings of the IEEE Conference on Computer Vision and Pattern Recognition* (pp. 472-480).
- [36] Simonyan, K., and Zisserman, A. (2014). Very deep convolutional networks for large-scale image recognition. *arXiv preprint arXiv:1409.1556*.
- [37] Yang, L. (2011). Classifiers selection for ensemble learning based on accuracy and diversity. *Procedia Engineering*, 15, 4266-4270.
- [38] Zhou, Z. H., Wu, J., and Tang, W. (2002). Ensembling neural networks: many could be better than all. *Artificial intelligence*, 137(1-2), 239-263.
- [39] Zhou, Z. H., and Tang, W. (2003, May). Selective ensemble of decision trees. In *International Workshop on Rough Sets, Fuzzy Sets, Data Mining, and Granular-Soft Computing* (pp. 476-483). Springer, Berlin, Heidelberg.
- [40] Kuncheva, L. I., and Whitaker, C. J. (2003). Measures of diversity in classifier ensembles and their relationship with the ensemble accuracy. *Machine learning*, 51(2), 181-207.
- [41] Neubeck, A., and Van Gool, L. (2006, August). Efficient non-maximum suppression. In *18th International Conference on Pattern Recognition (ICPR'06)* (Vol. 3, pp. 850-855). IEEE.
- [42] Chen, L., Liu, Z., Tong, L., Jiang, Z., Wang, S., Dong, J., and Zhou, H. (2020). Underwater object detection using Invert Multi-Class Adaboost with deep learning. *arXiv preprint arXiv:2005.11552*.
- [43] Redmon, J., and Farhadi, A. (2018). Yolov3: An incremental improvement. *arXiv preprint arXiv:1804.02767*.
- [44] Hoiem, D., Chodpathumwan, Y., and Dai, Q. (2012, October). Diagnosing error in object detectors. In *European Conference on Computer Vision* (pp. 340-353). Springer, Berlin, Heidelberg.
- [45] He, K., Zhang, X., Ren, S., and Sun, J. (2016). Deep residual learning for image recognition. In *Proceedings of the IEEE Conference on Computer Vision and Pattern Recognition* (pp. 770-778).

**Long Chen** is currently pursuing the PhD degree with the School of Informatics, University of Leicester, U.K. His research interests are in the areas of Computer Vision and Machine Learning.

**Feixiang Zhou** is currently pursuing the Ph.D. degree with the School of Informatics, University of Leicester, Leicester, U.K.

**Shengke Wang** is currently a Associate Professor of the Department of Computer Science and Technology, Ocean University of China, Qingdao, China.

**Junyu Dong** is currently a Professor and the Head of the Department of Computer Science and Technology, Ocean University of China, Qingdao, China.

**Ning Li** currently is an Associate Professor at College of Electronic and Information Engineering, Nanjing University of Aeronautics and Astronautics, China.

**Haiping Ma** is an Associate Professor at Department of Electrical Engineering, Shaoxing University, Shaoxing, Zhejiang, 312000, China.

**Xin Wang** is an Associate Professor at College of Computer and Information, Hohai University, China.

**Huiyu Zhou** currently is a Professor at School of Informatics, University of Leicester, United Kingdom.